AUTOMATIKA
2021, VOL. 62, NOS. 3–4, 520–529
https://doi.org/10.1080/00051144.2021.1991176

REGULAR PAPER

OPEN ACCESS Check for updates

Payload motion control for a varying length flexible gantry crane

Tung Lam Nguyen [a], Hong Quang Nguyen [b] and Minh Duc Duong [a]

[a]Hanoi University of Science and Technology, Hanoi, Vietnam; [b]Thai Nguyen University of Technology, Thai Nguyen, Vietnam

ABSTRACT

Cranes play a very important role in transporting heavy loads in various industries. However, because of its natural swinging characteristics, the control of crane needs to be considered carefully. This paper presents a control approach to a flexible cable crane system in consideration of both rope length varying and system constraints. At first, from Hamilton's extended principle the equations of motion that characterized coupled transverse-transverse motions with varying rope length of the gantry are obtained. The equations of motion consist of a system of partial differential equations. Then, a barrier Lyapunov function is used to derive the control located at the trolley end that can precisely position the gantry payload and minimize vibrations. The designed control is verified through extensive experimental studies.

ARTICLE HISTORY
Received 10 December 2019
Accepted 25 August 2021

KEYWORDS
Lyapunov stability; flexible system; vibration control; boundary control; gantry crane

1. Introduction

Overhead cranes are widely used in many applications such as manufacturing factories, marine industries and harbour operations, due to their capability of transporting heavy loads or hazardous materials. However, as a typical under-actuated system, and in some situations, rope flexible deformation cannot be ignored, the crane load is frequently swinging during transportation processes, which affects the positioning accuracy of the load, and brings danger, damage, even accidents in working sites. Thus, the main problem in handling the crane system is to reduce the sway angle of the load and moving it to a desired position with a fast motion.

Recently, various studies have been done to solve the above-mentioned problems. Many control strategies have been applied to the crane system that can be divided into three categories including open loop (such as input shaping, filtering, command smoothing), closed loop (such as classical linear control, intelligent control, optimal control, adaptive control, sliding mode control and so on), and combined open and closed loop control, see [1] for more details. In addition, several efforts to use some other control algorithms have been investigated. In [2], time-optimal flatness-based control has been used to minimize the transition time. Model predictive control in combination with disturbance predictor is used in [3] for control of the crane system with strong disturbances and uncertainties. In [4], the hybrid partial feedback linearization and deadbeat control scheme is applied to control the crane. In this research, a deadbeat control is used to control and accelerate the position response, while partial feedback linearization is in charge of minimizing and stabilizing the sway angle. Moreover, to delivery high-performance control operation for overhead crane, four control schemes are combined in [5] to control a overhead crane. The discrete-time controller is formulated based on state feedback approach to provide servo control operation. The reference signal generator based on typical anti-swing trajectory performed by an expert crane operator is used to supply reference state trajectory profiles. The feedforward control that generates the designed output trajectory from system model to reduce nonlinear disturbance and improve the tracking accuracy. Simultaneously, the load swing control that uses a high-gain observer to damp the load swings. To avoid the dependence of controller design on the crane model, a model-independent control called proportional-derivative with sliding mode control is proposed in [6]. The controller is model free that makes it robust with uncertain/unknown system parameters. In addition, to overcome the sensitivity of measured signal for feedback control scheme, inverse dynamic that uses simulations of feedback control by machine learning has been proposed in [7]. In this research, artificial neural network that can act in real-time is used to learn inverse dynamic model from actual crane.

All of aforementioned works treat crane motion as a pendulum-like system and the crane cable is assumed as a rigid body. However, the crane cable is flexible in practice, that assumption is not valid, especially in case of light loaded situations or underwater operations. This leads to a requirement of considering the flexibility of crane cable while designing the crane controller.

CONTACT Hong Quang Nguyen quang.nguyenhong@tnut.edu.vn

In [8], the overhead crane with a flexible cable is modelled as a hybrid partial differential equation - ordinary differential equation system. And a feedback stabilization controller is proposed to asymptotically stabilize the system. To obtain the exponential stabilization for the flexible cable crane system, cascade approach [9] and back-stepping approach [10] are applied. Some researchers have also designed controller for flexible cable crane based on Lyapunov theory such as in [11–13]. Boundary control for stabilizing the in-plane motion gantry crane system is introduced in [14, 15], where the problem mentioned in [15] consisting of two payloads that is not very common in practice. An interesting control solution for the overhead crane can be found in [16] where the authors consider delayed boundary condition, the closed loop system is proven to be well-posed and asymptotic stable. The dynamics of flexible cable are also described by the wave equation and a finite-time stabilization controller is designed for the crane in [17]. Moreover, control of the flexible cable crane with variable cable length is also considered in [18–20]. In these works, the authors concentrate to the ultimate goal which is achieving the payload to desired position and minimizing swinging angle in steady state. For certain applications when working space is limited, it is necessary to have a hard constraint on the payload motion especially in transient period.

In some certain applications, such as safety-critical systems, or mechanical stoppages, the violation of space constraints will cause serious hazards. Thus, dealing with payload vibration constrains might be necessary. The problem of above control schemes for the flexible cable crane have not considered the constraints. In order to overcome this obstacle, the concept of barrier Lyapunov function has been applied [21–23]. However, these systems use an additional boundary control force at payload that might be problematic in practice. The barrier Lyapunov function is also used in [24] to control the flexible cable crane with constraints in the face of non-varying rope length. However, none of above-mentioned works consider both variable cable length and payload constraints in controller design of flexible cable cranes.

The purpose of this research is to design a controller acting on trolley end for flexible cable with varying rope length crane that can precisely position the crane payload while minimize and retain the payload swinging motion in a predefined range for safety operation, this is also the main contribution of the paper. In order to obtain this purpose, the crane model with flexible and variable length cable is carefully derived. Then a control scheme is formulated from the proposed barrier Lyapunov function that stabilizes the system and takes the desired constraints in consideration. Experimental works are carried out to validate the effectiveness of the proposed controller.

2. Problem formulation

Before proceeding to derive mathematical model of the gantry crane, some important assumptions are specified as follows [20]:

Assumption: (1) The gantry crane operates and deforms in one plane only.
(2) Hooke's law is applied to the gantry cable elongation deformation.
(3) The system friction is totally ignored.
(4) Hook effect between the gantry cable and payload is not considered.
(5) The payload is modelled as a point-mass i.e. payload geometry is not taken into account.
(6) Deflection angle from vertical Z axis is very small.

Remark: Assumption 1 implies that single-beam gantry crane is considered. Assumption 2 indicates the gantry cable material is homogeneous, isotropic, and linearly elastic. Assumptions 3 and 4 emphasize the scope of the paper, system friction and hook effect will be our future concerns. Assumptions 4 and 6 generally hold in low capacity gantry cranes.

In order to formulate the dynamical model of a crane, we set the crane in a Cartesian coordinate system as shown in Figure 1. The crane includes a cart with weight m_T run along Ox axis. At time t, the cart is at position $x(t)$. The rope is with linear density ρ and a load with weight m_P is mounted at the rope's end. At a time t, the rope length is $l(t)$. There are two input forces, F_x, to move the cart, and F_l to lift the load. In practice, the forces are generated by torque controlled electric motors through mechanical gearing systems. In the

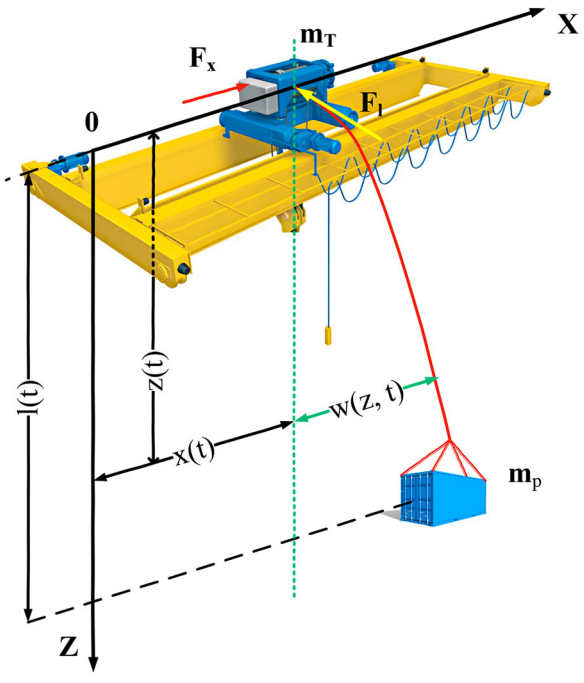

Figure 1. System coordinate.

paper scope, it is assumed that the electro-mechanical system is ideal. Hence, it is straightforward to consider acting forces F_x and F_l as control inputs. A point P in the rope at the time t can be expressed by it position along Oz axis $z(t)$, and the difference from the cart along Ox axis, $w(z(t), t)$. The point P can be described as $\vec{r}_p$ and is calculated as follows:

$$\vec{r}_p = [x(t) + w(t, z(t))]\vec{i} + z(t)\vec{k} \tag{1}$$

where $\vec{i}$ and $\vec{k}$ are unit vectors of Ox and Oz axes respectively. Then, velocity vector $\vec{v}_p$ at P can be calculated as

$$\vec{v}_p = [x_t(t) + w_t(z(t), t) + z_t(t)w_z(z(t), t)]\vec{i} + z_t(t)\vec{k} \tag{2}$$

where we have used the following notations

$$x_t = \frac{\mathrm{d}x(t)}{\mathrm{d}t};\ z_t = \frac{\mathrm{d}z(t)}{\mathrm{d}t};$$
$$w_t = \frac{\partial w(z(t), t)}{\partial t};\ w_z = \frac{\partial w(z(t), t)}{\partial z}.$$

Total kinetic energy KE of the system includes kinetic energy of the cart, rope and load, and can be calculated as follows:

$$KE = \frac{1}{2}\rho \int_0^{l(t)} [(x_t + w_t + z_t w_t)^2] + z_t^2]\mathrm{d}z + \frac{1}{2}m_T x_T^2 + \frac{1}{2}m_p[(x_t + \bar{w}_t + l_t\bar{w}_z)^2 + l^2] \tag{3}$$

with

$$\bar{w}_t = \frac{\partial w(z(t), t)}{\partial t}|_{z=l(t)};\ \bar{w}_z = \frac{\partial w(z(t), t)}{\partial z}|_{z=l(t)};$$
$$l_t = \frac{\mathrm{d}l(t)}{\mathrm{d}t}.$$

Total potential energy PE of the system includes potential energy of the cart, the rope, the load, and can be calculated as follows:

$$PE = \frac{1}{2}\int_0^{l(t)} [m_p g + \rho g(l - z)]w_z^2 \mathrm{d}z - m_p g l - \int_0^{l(t)} \rho g z\, \mathrm{d}z \tag{4}$$

with g is gravity acceleration. According to Hamilton's principle

$$\int_{t_1}^{t_2} (\delta KE - \delta PE + \delta W)\, \mathrm{d}t = 0 \tag{5}$$

with W is the work done by external forces and $\delta W = F_x\delta_x + F_l\delta_l$. Substitute (3) and(4) into (5), and set

$$L_c = \frac{1}{2}\rho[(x_t + w_t + z_t w_t)^2 + z_t^2] - \frac{1}{2}Tw_z^2 + \rho g z = L_c(t; x_t, z, z_t, w_t, w_z) \tag{6}$$

$$L_m = \frac{1}{2}m_p[(x_t + \bar{w}_t + l_t\bar{w}_z)^2 + l_t^2] + \frac{1}{2}m_T x_t^2 + m_p g l = L_m(t; x_t, l, l_t, \bar{w}_t, \bar{w}_z) \tag{7}$$

where $T = m_p g + \rho g(l - z)$ is the cable tension. Equation (5) can be rewritten in a compact form as

$$\int_{t_1}^{t_2} \left[\delta \int_0^{l(t)} L_c\, \mathrm{d}z + \delta L_m + F_x\delta_x + F_l\delta_l\right] \mathrm{d}t = 0 \tag{8}$$

The variation of L_c can be calculated as

$$\delta \int_0^{l(t)} L_c\, \mathrm{d}z = L_c\delta z|_{z=0}^{z=l(t)} + \int_0^{l(t)} \delta L_c\, \mathrm{d}z = \bar{L}_c\delta l(t) + \int_0^{l(t)} \delta L_c\, \mathrm{d}z \tag{9}$$

where $\bar{L}_c = L_c|_{z=l(t)}$. In addition, it is straight forward to yield

$$\delta L_c = \frac{\partial L_c}{\partial x_t}\delta x_t + \frac{\partial L_c}{\partial z}\delta z + \frac{\partial L_c}{\partial z_t}\delta z_t + \frac{\partial L_c}{\partial w_t}\delta w_t + \frac{\partial L_c}{\partial w_z}\delta w_z \tag{10}$$

and

$$\int_0^{l(t)} \delta L_c = \int_0^{l(t)} \left[\frac{\partial L_c}{\partial x_t}\delta x_t + \frac{\partial L_c}{\partial z}\delta z + \frac{\partial L_c}{\partial z_t}\delta z_t + \frac{\partial L_c}{\partial w_t}\delta w_t + \frac{\partial L_c}{\partial w_z}\delta w_z\right] \mathrm{d}z. \tag{11}$$

Moreover using integration by parts, it can be shown that

$$\int_0^{l(t)} \frac{\partial L_c}{\partial w_z}\delta w_z\, \mathrm{d}z = \left[\frac{\partial L_c}{\partial w_z}(\delta w)\right]\Big|_0^{l(t)} - \int_0^{l(t)} \left(\frac{\partial L_c}{\partial w_z}\right)_z \delta w\, \mathrm{d}z \tag{12}$$

From (11) and (12), we can obtain

$$\int_{t_1}^{t_2} \left(\int_0^{l(t)} \delta L_c \mathrm{d}z\right) \mathrm{d}t = \int_{t_1}^{t_2} \left\{\int_0^{l(t)} \left[\frac{\partial L_c}{\partial x_t}\delta x_t + \frac{\partial L_c}{\partial z}\delta z + \frac{\partial L_c}{\partial z_t}\delta z_t + \frac{\partial L_c}{\partial w_t}\delta w_t - \left(\frac{\partial L_c}{\partial w_z}\right)_z\right] \mathrm{d}z + \left[\frac{\partial L_c}{\partial w_z}(\delta w)\right]\Big|_0^{l(t)}\right\} \mathrm{d}t \tag{13}$$

For the sake of simplicity in the presentation, let us calculate each single term in (13)

$$\int_{t_1}^{t_2} \left\{\int_0^{l(t)} \left[\frac{\partial L_c}{\partial x_t}\delta x_t\right] \mathrm{d}z\right\} \mathrm{d}t$$

$$= \int_0^{l(t)} \left\{ \int_{t_1}^{t_2} \left[\frac{\partial L_c}{\partial x_t} \frac{\mathrm{d}(\delta x)}{\mathrm{d}t} \right] \mathrm{d}t \right\} \mathrm{d}z$$
$$= \int_0^{l(t)} \left\{ \int_{t_1}^{t_2} \left[\frac{\partial L_c}{\partial x_t} \mathrm{d}(\delta x) \right] \right\} \mathrm{d}z$$
$$= \int_0^{l(t)} \left[\frac{\partial L_c}{\partial x_t} (\delta x) \right] \Big|_{t_1}^{t_2} - \int_0^{l(t)} \left\{ \int_{t_1}^{t_2} \left[\frac{\mathrm{d}}{\mathrm{d}t} \left(\frac{\partial L_c}{\partial x_t} \right) \delta x \right] \mathrm{d}t \right\} \mathrm{d}z$$
$$= - \int_0^{l(t)} \left\{ \int_{t_1}^{t_2} \left[\frac{\mathrm{d}}{\mathrm{d}t} \left(\frac{\partial L_c}{\partial x_t} \right) \delta x \right] \mathrm{d}t \right\} \mathrm{d}z \quad (14)$$

Similarly, we also have

$$\int_{t_1}^{t_2} \left\{ \int_0^{l(t)} \left[\frac{\partial L_c}{\partial z_t} \delta z_t \right] \mathrm{d}z \right\} \mathrm{d}t = - \int_{t_1}^{t_2} \left\{ \int_0^{l(t)} \left[\frac{\mathrm{d}}{\mathrm{d}t} \left(\frac{\partial L_c}{\partial z_t} \right) \delta z \right] \mathrm{d}z \right\} \mathrm{d}t \quad (15)$$

$$\int_{t_1}^{t_2} \left\{ \int_0^{l(t)} \left[\frac{\partial L_c}{\partial w_t} \delta w_t \right] \mathrm{d}z \right\} \mathrm{d}t = - \int_{t_1}^{t_2} \left\{ \int_0^{l(t)} \left[\frac{\mathrm{d}}{\mathrm{d}t} \left(\frac{\partial L_c}{\partial w_t} \right) \delta w \right] \mathrm{d}z \right\} \mathrm{d}t \quad (16)$$

Substitute (14)–(16) into 17 we obtain

$$\int_{t_1}^{t_2} \left(\int_0^{l(t)} \delta L_c \mathrm{d}z \right) \mathrm{d}t = \int_{t_1}^{t_2} \left\{ \int_0^{l(t)} \left[-\frac{\mathrm{d}}{\mathrm{d}t} \left(\frac{\partial L_c}{\partial x_t} \right) \delta x - \frac{\mathrm{d}}{\mathrm{d}t} \left(\frac{\partial L_c}{\partial z_t} \right) \delta z - \frac{\mathrm{d}}{\mathrm{d}t} \left(\frac{\partial L_c}{\partial w_t} \right)_t \delta w - \left(\frac{\partial L_c}{\partial w_z} \right)_z \delta w + \frac{\partial L_c}{\partial z} \delta z \right] \mathrm{d}z + \left[\frac{\partial L_c}{\partial w_z} \delta w \right] \Big|_0^{l(t)} \right\} \mathrm{d}t \quad (17)$$

We also have

$$\delta L_m = \delta L_m(t; x_t, l, l_t, \bar{w}_t, \bar{w}_z) = \frac{\partial L_m}{\partial x_t} \delta x_t + \frac{\partial L_m}{\partial l} \delta l + \frac{\partial L_m}{\partial l_t} \delta l_t + \frac{\partial L_m}{\partial \bar{w}_t} \delta \bar{w}_t + \frac{\partial L_m}{\partial \bar{w}_z} \delta \bar{w}_z, \quad (18)$$

then, by calculating as same as with L_c, we can obtain

$$\int_{t1}^{t2} \delta L_m \mathrm{d}t = \int_{t1}^{t2} \left[-\frac{\mathrm{d}}{\mathrm{d}t} \frac{\partial L_m}{\partial x_t} \delta x + \frac{\partial L_m}{\partial l} \delta l - \frac{\mathrm{d}}{\mathrm{d}t} \frac{\partial L_m}{\partial l_t} \delta l - \left(\frac{\partial L_m}{\partial \bar{w}_t} \right)_t \delta \bar{w}_t + \frac{\partial L_m}{\partial \bar{w}_z} \delta \bar{w}_z \right] \mathrm{d}t \quad (19)$$

Because of $w_z^2 << 1, \delta z = \delta l$, substituting (17) and (19) into (9) yields

$$\int_{t1}^{t2} \left\{ - \int_0^{l(t)} \left[\left(\frac{\partial L_c}{\partial w_t} \right)_t + \left(\frac{\partial L_c}{\partial w_z} \right)_z \right] \mathrm{d}z \delta w - \left[\int_0^{l(t)} \frac{\mathrm{d}}{\mathrm{d}t} \frac{\partial L_c}{\partial x_t} \mathrm{d}z + \frac{\mathrm{d}}{\mathrm{d}t} \frac{\partial L_m}{\partial x_t} - F_x \right] \delta x - \left[\int_0^{l(t)} \left[\frac{\mathrm{d}}{\mathrm{d}t} \frac{\partial L_c}{\partial z_t} - \frac{\partial L_c}{\partial z} \right] \mathrm{d}z - \bar{L}_c + \frac{\mathrm{d}}{\mathrm{d}t} \frac{\partial L_m}{\partial l_t} - \frac{\partial L_m}{\partial l} - F_l \right] \delta l + \left[\frac{\partial L_c}{\partial w_z} \Big|_{z=l(t)} - \left(\frac{\partial L_m}{\partial \bar{w}_t} \right)_t \right] \delta \bar{w} - \frac{\partial L_c}{\partial w_z} \Big|_{z=0} \delta w(0,t) + \frac{\partial L_m}{\partial \bar{w}_z} \delta \bar{w}_z \right\} \mathrm{d}t = 0 \quad (20)$$

Since t_1 and t_2 are arbitrarily, (20) implies

$$\left(\frac{\partial L_c}{\partial w_t} \right)_t + \left(\frac{\partial L_c}{\partial w_z} \right)_z = 0 \quad (21)$$

$$\text{and} \int_0^{l(t)} \frac{\mathrm{d}}{\mathrm{d}t} \frac{\partial L_c}{\partial x_t} \mathrm{d}z + \frac{\mathrm{d}}{\mathrm{d}t} \frac{\partial L_m}{\partial x_t} = F_x \quad (22)$$

$$\text{and} \int_0^{l(t)} \left[\frac{\mathrm{d}}{\mathrm{d}t} \frac{\partial L_c}{\partial z_t} - \frac{\partial L_c}{\partial z} \right] \mathrm{d}z - \bar{L}_c + \frac{\mathrm{d}}{\mathrm{d}t} \frac{\partial L_m}{\partial l_t} - \frac{\partial L_m}{\partial l} = F_l \quad (23)$$

$$\text{and} \left. \frac{\partial L_c}{\partial w_z} \right|_{z=0} \delta w(0,t) = 0 \quad (24)$$

$$\text{and} \left. \frac{\partial L_c}{\partial w_z} \right|_{z=l(t)} - \left(\frac{\partial L_m}{\partial \bar{w}_t} \right)_t = 0 \quad (25)$$

Equation (21) represents the motion of the cable, a simple operation give a more detailed form of the equation of motions as

$$\rho(x_{tt} + w_{tt} + z_{tt} w_z + z_t(2w_{zt} + w_{zz})) = (Tw_z)_z \quad (26)$$

It is noted that we have used the following notation

$$x_{tt} = \frac{\partial^2 x}{\partial t^2}, \; w_{tt} = \frac{\partial^2 w}{\partial t^2}, \; z_{tt} = \frac{\partial^2 z}{\partial t^2},$$

and

$$w_{zt} = \frac{\partial^2}{\partial z \partial r}.$$

Similar approach yields from (22)

$$F_x = \int_0^{l(t)} \rho(x_{tt} + w_{tt} + z_{tt} w_z + z_t(2w_{zt} + z_t w_{zz})) \mathrm{d}z + m_T x_{tt} + m_p(x_{tt} + \bar{w}_{tt} + l_{tt} \bar{w}_z + l_t(2\bar{w}_{zt} + l_t \bar{w}_{zz})) \quad (27)$$

and from(23), performing integration by parts shows that

$$\begin{aligned}\bar{F}_l &= F_l + m_p g + \rho g l \\ &= \int_0^{l(t)} \big(\rho((x_{tt} + w_{tt} + z_{tt}w_z + z_t(2w_{zt} \\ &\quad + z_t w_{zz}))w_z + Tw_z w_{zz}\big)\mathrm{d}z \\ &\quad + m_p((x_{tt} + \bar{w}_{tt} \\ &\quad + l_{tt}\bar{w}_z + l_t(2\bar{w}_{zt} + l_t\bar{w}_{zz}))\bar{w}_z + l_{tt} \\ &\quad - \frac{1}{2}\rho((x_t + \bar{w}_t) + l_t\bar{w}_z)^2 + l_t^2) + \frac{1}{2}m_p g\bar{w}_z^2\end{aligned} \tag{28}$$

Equations (27) and (28) characterize the relation between control forces and the transverse, hoisting motions, respectively. The relation will be used to further in control design step. Equation (24) simply becomes

$$w(0,t) = 0 \tag{29}$$

Carefully applying time and spatial derivatives, (25) simply turns into

$$\begin{aligned}&\rho(x_t + \bar{w}_t + l_t\bar{w}_z)l_t - m_p g\bar{w}_z \\ &\quad - m_p(x_{tt} + \bar{w}_{tt} + l_t(2\bar{w}_{zt} + l_t\bar{w}_{zz})) = 0\end{aligned} \tag{30}$$

Equations (26)–(30) describe the dynamical model of a crane system with varying cable length. Based on the dynamics of the cable and boundary conditions, a variant of traditional Lyapunov function will be employed to develop the position and vibration controller for the system.

3. Position and vibration control design

Since the input forces are applied at the trolley end of the system, the control design process has to guarantee the location of the inputs, minimize and retain the payload swinging motion in a predefined range. In order to achieve the control objective, the direct Lyapunov method is employed. Considering the following Lyapunov candidate function given as

$$\begin{aligned}V_1(t) &= \frac{1}{2}\int_0^{l(t)} \big(\rho[(x_t + w_t + z_t w_z)^2 + z_t^2] + Tw_z^2\big)\mathrm{d}z \\ &\quad + \frac{1}{2}m_p[(x_t + \bar{w}_t + l_t\bar{w}_z)^2 + l_t^2 \\ &\quad + \frac{1}{2}k_1 m_T x_t^2 + \frac{1}{2}k_2(x - x_d)^2 + \frac{1}{2}k_3(l - l_d)^2 \\ &\quad + \frac{k_c}{2}\log\left(\frac{k_b^2}{k_b^2 - \bar{w}^2}\right)\end{aligned} \tag{31}$$

where k_b is a positive constant denoting a distance defined range that constraining the payload motion and k_c is a positive constant. We assume that at the initial condition $w(z,0) < k_b$, which generally holds in practice. Compare to the conventional Lyapunov approach which includes system energy and tracking errors, the natural logarithm term $\log(\bullet)$ is embedded to tackle the the requirement of maintaining the payload in a certain distance from the equilibrium position. The first derivative of $V_1(t)$ with time t is calculated as follows:

$$\begin{aligned}\dot{V}(t) &= \frac{1}{2}\int_0^{l(t)} \big((2\rho(x_t + w_t + z_t w_z) \\ &\quad \times (x_{tt} + w_{tt} + z_{tt}w_z + z_t(2w_{zt}z_t w_{zz})) + 2z_t z_{tt} \\ &\quad + 2Tw_z w_{zz}z_t + 2Tw_{zt}w_z\big)\,\mathrm{d}z \\ &\quad + \frac{1}{2}\rho l_t\big((\bar{x}_t\bar{w}_t + l_t\bar{w}_z)^2 + l_t^2\big) \\ &\quad + m_p g\bar{w}_z^2 + k - 1m_T x_t x_{tt} \\ &\quad + m_p\big((x_t\bar{w}_t + l_t\bar{w}_z) \\ &\quad \times (x_{tt}\bar{w}_{tt} + l_{tt}\bar{w}_z + l_t(2\bar{w}_{zt} + l_t w_{zz})) + l_t l_{tt}\big) \\ &\quad + k_2(x - x_d)x_t + k_3(l - l_d)l_t + k_c\frac{\bar{w}\bar{w}_t}{k_b^2 - \bar{w}}\end{aligned} \tag{32}$$

Fundamental operations show that

$$\begin{aligned}\dot{V}(t) &= k_1\int_0^{l(t)} \rho x_t\big(x_{tt} + w_{tt} + z_{tt}w_z \\ &\quad + z_t(2w_{zt} + z_t w_{zz})\big)\,\mathrm{d}z + k_1 m_T x_t x_{tt} \\ &\quad + k_1 m_P x_t\big(x_{tt} + \bar{w}_{tt} + l_{tt}\bar{w}_z + l_t(2\bar{w}_{zt} + l_t w_{tt})\big) \\ &\quad + k_2(x - x_d)x_t + \int_0^{l(t)} \Big(\rho w_z z_t\big(x_{tt} + w_{tt} \\ &\quad + z_{tt}w_z + z_t(2w_{zt} + z_t w_{zz})\big) \\ &\quad + z_t z_{tt} + Tw_z w_{zz}z_t + Tw_{zt}w_z\Big)\mathrm{d}z \\ &\quad + m_P l_t w_z\Big(\big(x_{tt} + \bar{w}_{tt} \\ &\quad + l_{tt}\bar{w}_z + l_t(w\bar{w}_{zt} + l_t w_{zz})\big) + l_{tt}\Big) \\ &\quad - \frac{1}{2}\rho l_t\big((x_t + \bar{w}_t + l_t\bar{w}_z)^2 + l_t^2\big) \\ &\quad + \frac{1}{2}m_P g\bar{w}_z^2 + k_3(l - l_d)l_t \\ &\quad + \int_0^{l(t)} \rho w_t\big(x_{tt} + w_{tt} + z_{tt}w_z \\ &\quad + z_t(2w_{zt} + z_t w_{wt})\big)\mathrm{d}z \\ &\quad + m_P\bar{w}_t\big(x_{tt} + \bar{w}_{tt} + l_{tt}\bar{w}_z + l_t(2\bar{w}_{zt} + l_t\bar{w}_{zz})\big) \\ &\quad + \rho l_t\big((x_t + \bar{w}_t + l_t\bar{w}_z)^2 + l_t^2\big) \\ &\quad + (1 - k_1)\int_0^{l(t)} \rho x \\ &\quad - t\big(x_{tt} + w_{tt} + z_{tt}w_z + z_t(2w_{zt} + z_t w_{zz})\big)\mathrm{d}z \\ &\quad + (1 - k_1)m_P x_t\big(x_{tt} - \bar{w}_{tt}\end{aligned}$$

$$+ l_{tt}\bar{w}_z + l_t(2\bar{w}_{zt} + l_t w_{zz})\big) + k_c\frac{\bar{w}}{k_b^2 - \bar{a}^2} \times (\bar{w}_t + l_t\bar{w}_z) \tag{33}$$

Using dynamic model (26)–(30) and integration by parts show that

$$\begin{aligned}\dot{V}_1(t) = {} & k_1F_x x_t + k_2(x - x_d)x_t + \bar{F}_l l_t \\ & + \int_0^{l(t)} w_t(Tw_z)_z dz + \int_0^{l(t)} Tw_{zt}w_z\,dz \\ & + \rho\bar{w}_t(x_t + \bar{w}_t + l_t\bar{w}z)l_t \\ & - m_p g\bar{w}_t\bar{w}_z + \rho l_t\big((x_t + \bar{w}_t + l_t\bar{w}_z)^2 + l_t^2\big) \\ & + (1 - k_1)\int_0^{l(t)} x_t(Tw_z)_z dz \\ & + (1 - k_1)x_t\big(\rho(x_t + \bar{w}_t + l_t\bar{w}_z)l_t - m_p g\bar{w}_z\big) \\ & + k_c\frac{\bar{w}}{k_b^2 - \bar{w}^2}(\bar{w}_t + l_t\bar{w}_z)\end{aligned} \tag{34}$$

Since $\bar{w}_t + l_t\bar{w}_z \le |\bar{w}_t + l_t\bar{w}_z|$, it can be deduced that

$$\begin{aligned}\dot{V}_1(t) = {} & k_1F_x x_t + k_2(x - x_d)x_t + \bar{F}_l l_t \\ & + \int_0^{l(t)} w_t(Tw_z)_z\,dz + \int_0^{l(t)} Tw_{zt}w_z\,dz \\ & + \rho\bar{w}_t(x_t + \bar{w}_t + l_t\bar{w}z)l_t - m_p g\bar{w}_t\bar{w}_z \\ & + \rho l_t\big((x_t + \bar{w}_t + l_t\bar{w}_z)^2 + l_t^2\big) \\ & + (1 - k_1)\int_0^{l(t)} x_t(Tw_z)_z\,dz \\ & + (1 - k_1)x_t\big(\rho(x_t + \bar{w}_t + l_t\bar{w}_z)l_t - m_p g\bar{w}_z\big) \\ & + k_c\frac{\bar{w}}{k_b^2 - \bar{w}^2}|\bar{w}_t + l_t\bar{w}_z|\end{aligned} \tag{35}$$

There exists a positive constant k_0 such that $|\bar{w}_t| \le k_0 x_t^2$, this implies that

$$|\bar{w}_t + l_t\bar{w}_z| \le |\bar{w}_t| + |l_t\bar{w}_z| + \text{sign}(l_t)l_t|\bar{w}_z| \tag{36}$$

Since $|\bar{w}| < k_b$, [25], we have

$$k_c\frac{\bar{w}}{k_b^2 - \bar{w}^2}|\bar{w}_t + l_t\bar{w}_z| \le K_c(k_0x_t^2 + \text{sign}(l_t)|\bar{w}_z|) \tag{37}$$

where $K_c = k_c\frac{k_b}{k_b^2 - \bar{w}^2}$. Inequality (37) suggests that (34) can be rewritten as

$$\begin{aligned}\dot{V}_1(t) \le {} & k_1F_x x_t + k_2(x - x_d)x_t + \bar{F}_l l_t \\ & + \int_0^{l(t)} w_t(Tw_z)_z\,dz + \int_0^{l(t)} Tw_{zt}w_z\,dz \\ & + \rho\bar{w}_t(x_t + \bar{w}_t + l_t\bar{w}z)l_t - m_p g\bar{w}_t\bar{w}_z \\ & + \rho l_t\big((x_t + \bar{w}_t + l_t\bar{w}_z)^2 + l_t^2\big) \\ & + (1 - k_1)\int_0^{l(t)} x_t(Tw_z)_z\,dz + (1 - k_1)x_t \\ & \times \big(\rho(x_t + \bar{w}_t + l_t\bar{w}_z)l_t - m_p g\bar{w}_z\big) \\ & + K_c(k_0x_t^2 + \text{sign}(l_t)|\bar{w}_z|)\end{aligned} \tag{38}$$

Applying integration by parts on tension related terms leads to

$$\int_0^{l(t)} w_t(Tw_z)_z\,dz = w_t Tw_z|_0^{l(t)} - \int_0^{l(t)} w_{zt}Tw_z\,dz \tag{39}$$

and

$$\int_0^{l(t)} x_t(Tw_z)_z z\,dz = m_P g x_t\bar{w}_z - (x_t Tw_z)_0 \tag{40}$$

Substituting (39), (40) into (38), and rearranging (38) lead to

$$\begin{aligned}\dot{V}(t) \le {} & [\bar{F}_l + k_3(l - l_d) + \rho\big((x_t + \bar{w}_t + l_t\bar{w}_z)^2 + l_t^2\big) \\ & + \rho(x_t + \bar{w}_t + l_t\bar{w}_z)\big(\bar{w}_t + (1 - k_1)x_t\big) \\ & + |\bar{w}_z|\text{sign}(l_t)K_c]l_t + [k_1F_x + k_2(x - x_d) \\ & - (1 - k_1)(Tw_z)|_{z=0} + K_c k_0 x_t]x_t\end{aligned} \tag{41}$$

At this step, recall the relation between input forces and system dynamics given in (27) and (28), the control can be selected as

$$\begin{aligned}\bar{F}_l = {} & -k_3(l - l_d) - \rho((x_t + \bar{w}_t + l_t\bar{w}_z)^2 + l_t^2) \\ & - \rho(x_t + \bar{w}_t + l_t\bar{w}_z)(\bar{w}_t + (1 - k_1)x_t) \\ & - k_l l_t + K_c|\bar{w}_z|\text{sign}(l_t)\end{aligned}$$

and

$$\begin{aligned}F_x = {} & -\frac{1}{k_1}[-k_2(x - x_d) + (1 - k_1)(Tw_z)|_{z=0} \\ & - k_x x_t - K_c k_0 x_t]\end{aligned} \tag{42}$$

The control input render $\dot{V}(t)$ as

$$\dot{V}_1(t) \le k_l l_t^2 - k_x x_t^2 \le 0 \tag{43}$$

Since $\dot{V}(t) \le 0$ and $V(t)$ is a function of $\bar{w}$, we conclude that $V(\bar{w})$ is bounded. Due to the assumption $w(z, 0) < k_b$ it implies that $|\bar{w}| < k_b \forall t$. It is noted that the designed controls require cable ends information that are available for feedback. The controls are totally applicable when embedding in actuators such as electric motors in torque control mode.

4. Experimental results

The ability of maintaining payload in a certain gap is illustrated in this section via a set of experiments. The gantry crane scaled model is depicted in Figure 2. The crane is designed to operate in three-dimensional space and its motions are actuated by three servo motors working in torque control mode combined with gearbox/rack and pinion transmissions Figure 2(a). The proposed controls are calculated and transformed

into required torque at the motor ends. Torque reference values are set through analog inputs of the servo drives in form of voltage. Payload swinging motion is detected by a special mechanism and converted into voltage signal that is proportional to payload fluctuation Figure 2(b).

Firstly, we only apply position control of the trolley to the system, payload fluctuation control is not activated. The PI position controller in tuned in such a way that desired trolley position is tracked when payload dynamic is removed. In this circumstance, system responses with different rope lengths and payload

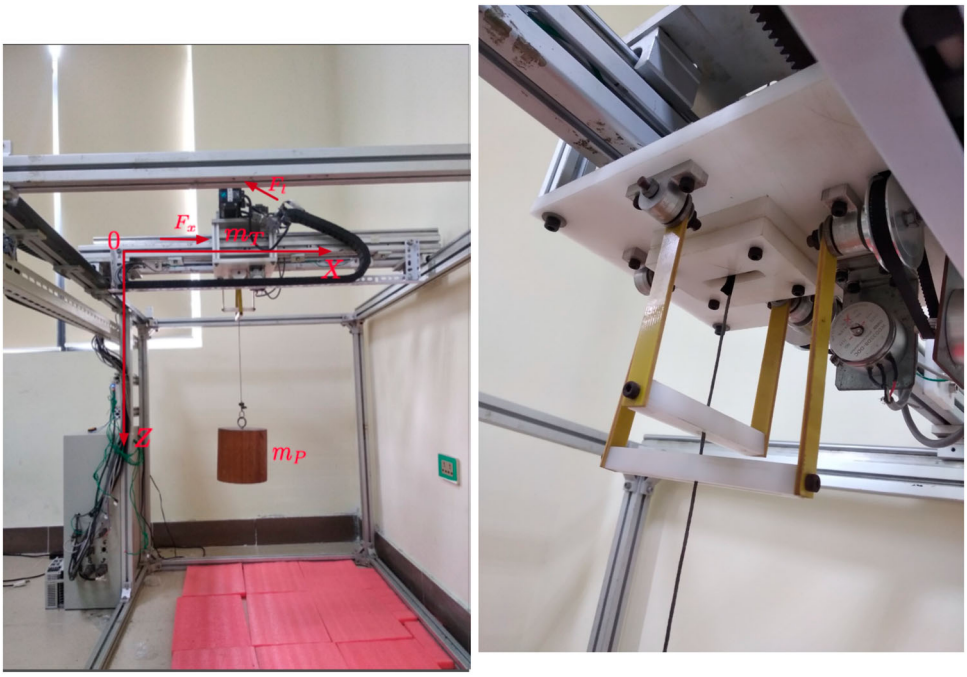

(a) (b)

Figure 2. Experiment setup: (a) 3D gantry crane model and (b) Payload swing angle measurement unit. (a) experiment1, (b) experiment2.

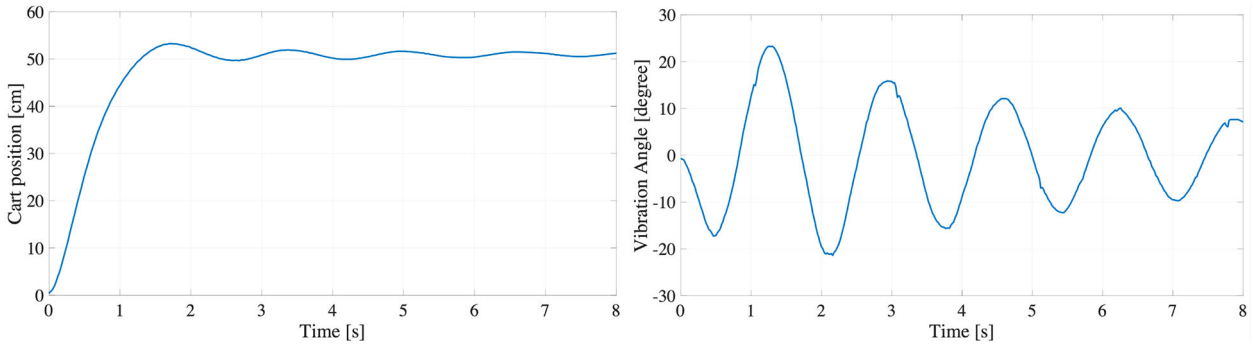

(a) (b)

Figure 3. System response with trolley position control $l = 0.5$ m, $m_p = 3$ kg: (a) Trolley motion and (b) Payload swinging angle.

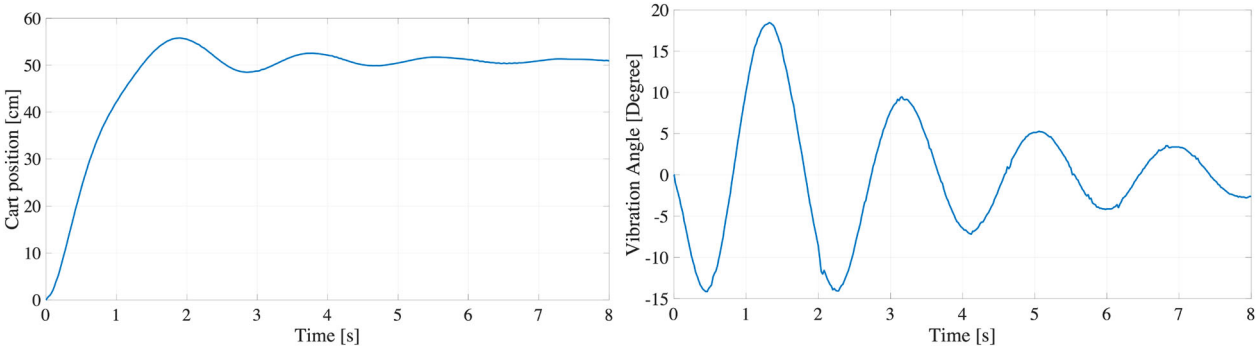

(a) (b)

Figure 4. System response with trolley position control ($l = 0.7$ m, $m_p = 5$ kg): (a) Trolley motion and (b) Payload swinging angle.

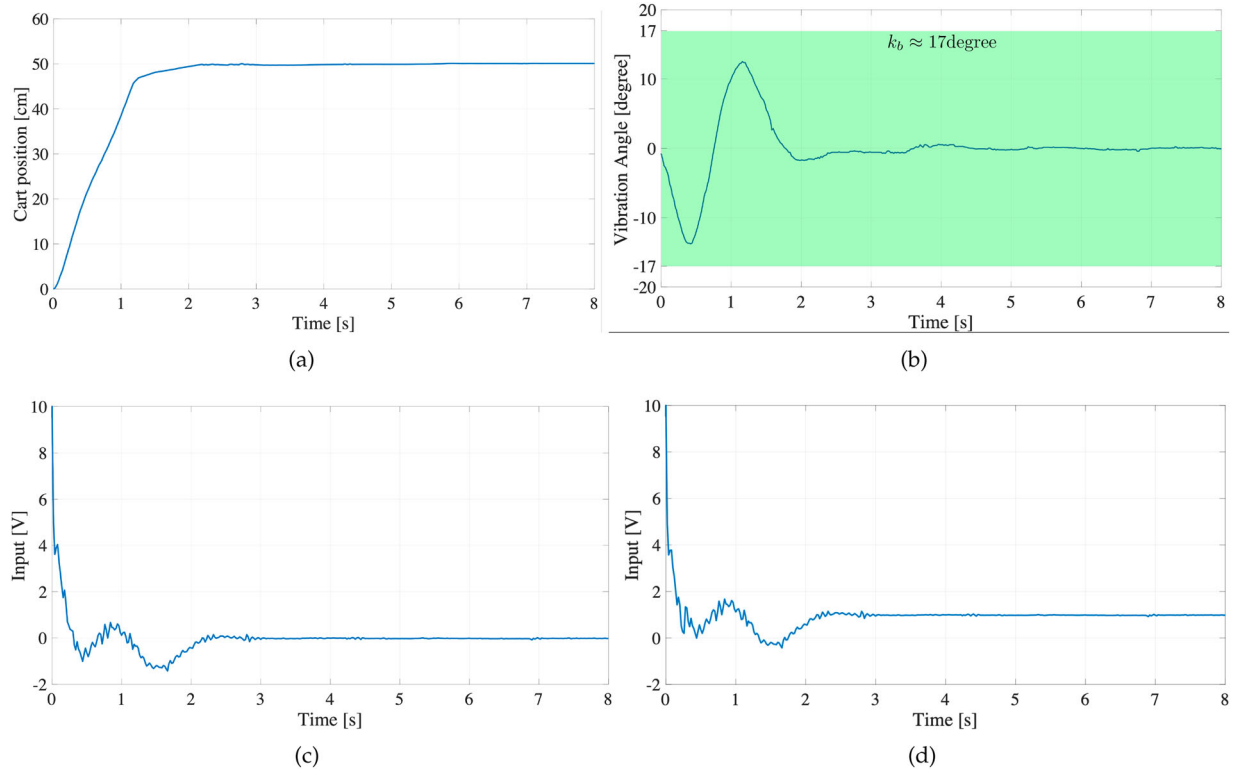

Figure 5. System response with the position and vibration control ($m_P = 3$ kg): (a) Trolley motion, (b) Payload swinging angle, (c) Input force F_x, and (d) Input force F_I.

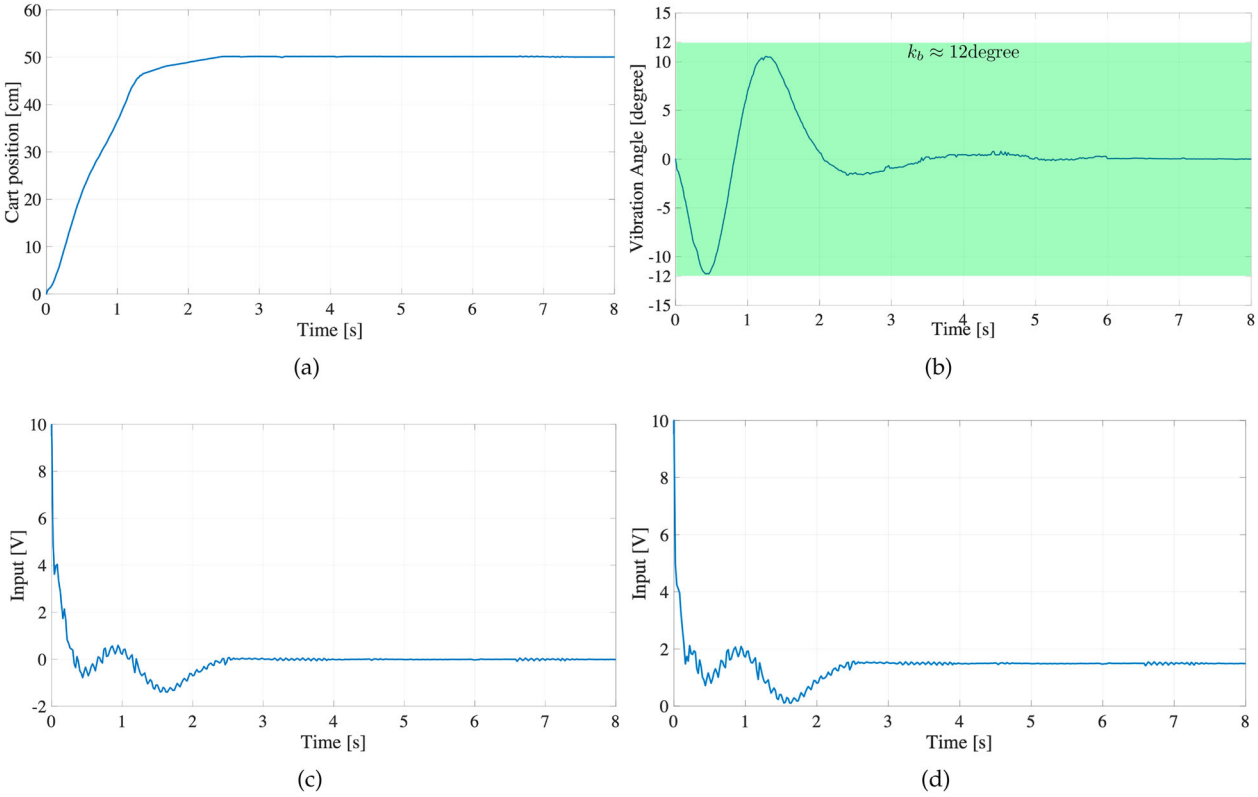

Figure 6. System response with the position and vibration control ($m_P = 5$ kg): (a) Trolley motion, (b) Payload swing angle, (c) Input force F_x, and (d) Input force F_I.

mass ($l = 0.5$ m, $m_p = 3$ kg and $l = 0.7$ m, $m_p = 5$ kg) are given in Figures 3 and 4, respectively. It can be seen that, without payload vibration suppression, payload fluctuation angle can reach approximately 25 degree when $l = 0.5$ cm, $m_p = 3$ kg. Lower vibration amplitude is witnessed in the case of $m_p = 5$ kg due to higher payload inertia. The vibration affects trolley responses as can be observed in Figure 3(a) and 4(a).

In the second experimental scenario, the integrated trolley position and payload vibration suppression proposed in the paper is activated. The control parameters are $k_l = 3, k_4 =, k_2 = 5, k_3 = 10, k_x = 8, k_b = 0.15$, this implies that the payload is to be maintained in a distance of 0.15 m away from the trolley vertical axis, and $k_c = 7$. At first, the payload is positioned at (0 m, 0.5 m) and then proceeds to (0.5, 0.5 m) and to (0.5, 0.7 m). Figure 5 and 6 present the system performances with $l = 0.5$ m, $m_p = 3$ kg and $l = 0.7$ m, $m_p = 5$ kg, respectively.

It can be observed from Figure 5 and 6 that under control action, payload vibration is considerably reduced. Payload maximum swinging angles for $l = 0.5$ m, $m_p = 3$ kg, and $l = 0.7$ m, $m_p = 5$ kg are at about 13 degree and 12 degree, respectively. Assuming pendulum-like motion of the crane system and applying simple trigonometric operations, it is can be shown that the payload motion in well maintained in a range defined by k_b which is corresponding to payload swinging angles of 17 degree and 12 degree, respectively. Control inputs are illustrated in Figures 5(c-d) and Figures 6(c-d). The experiment shows the effectiveness of the proposed control based on the application of barrier Lyapunov function where payload motion from the trolley axis is well kept in the area defined by k_b.

5. Conclusions

Due to the tremendous applications in different fields, gantry crane dynamics and control draw researchers attention. In this paper, the problem of position and vibration suppression in the gantry crane system with variable length flexible cable and payload motion constraints are considered. The system was represented by partial differential equation model from Hamilton's extended principle. Based on the novel barrier Lyapunov function, the control scheme that stabilize the crane system has been derived. Moreover, the payload has been successfully moved to the desired point, vibrations of the variable flexible cable have been greatly suppressed, and the boundary payload motion constraint has been satisfied. Experimental results have been provided to verify the performance of the proposed control. However, the well-posed problem of the designed controller is not proven. The crane system consider is placed on a solid foundation, our future works will look at dynamics and control aspects of the system mounted on moving foundation in ship-to-ship and ship-to-shore operations.

Disclosure statement

No potential conflict of interest was reported by the author(s).

Funding

This research is funded by Hanoi University of Science and Technology (HUST) under project number T2021-PC-001.

ORCID

Tung Lam Nguyen http://orcid.org/0000-0003-4108-8275
Hong Quang Nguyen http://orcid.org/0000-0002-0433-3094
Minh Duc Duong http://orcid.org/0000-0003-1057-0632

References

[1] Ramli L, Mohamed Z, Abdullahi AM, et al. Control strategies for crane systems: a comprehensive review. Mech Syst Signal Process. 2017;95:1–23.
[2] Kolar B, Rams H, Schlacher K. Time-optimal flatness based control of a gantry crane. Control Eng Pract. 2017 Mar;60(2016):18–27.
[3] Ma X, Bao H. An anti-swing closed-loop control strategy for overhead cranes. Appl Sci. 2018;8(9). https://doi.org/10.3390/app8091463
[4] Hamdy M, Shalaby R, Sallam M. A hybrid partial feedback linearization and deadbeat control scheme for a nonlinear gantry crane. J Franklin Inst. 2018;355(14):6286–6299.
[5] Khatamianfar A, Savkin AV. Real-time robust and optimized control of a 3D overhead crane system. Sensors. 2019;19(15). doi:10.3390/s19153429
[6] Zhang M, Zhang Y, Chen H, et al. Model-independent PD-SMC method with payload swing suppression for 3D overhead crane systems. Mech Syst Signal Process. 2019;129:381–393.
[7] Rincon L, Kubota Y, Venture G, et al. Inverse dynamic control via simulation of feedback control by artificial neural networks for a crane system. Control Eng Pract. 2020 Nov;94(2019). doi:10.1016/j.conengprac.2019.104203
[8] Andrea-Novel BD, Boustany F, Conrad F, et al. Feedback stabilization of a hybrid PDE-ODE system: application to an overhead crane. Math Control Signals Syst. 1994;7(1):1–22.
[9] D'Andrea-Novel B, Coron J. Exponential stabilization of an overhead crane with flexible cable via the cascade approach. IFAC Proc Vol. 1997;30(20):569–576.
[10] D'Andrea-Novel B, Coron JM. Exponential stabilization of an overhead crane with flexible cable via a backstepping approach. Automatica. 2000;36(4):587–593.
[11] Abdelhadi E. Exponential stabilization and motion planning of an overhead crane system. IMA J Math Control Inf. 2017;34(4):1299–321. doi:10.1093/imamci/dnw026.
[12] Joshi S, Rahn CD. Position control of a flexible cable gantry crane: theory and experiment. Proc Am Control Conf. 1995 Jun;4(4):2820–2824. doi:10.1093/imamci/dnw026.

[13] Kim CW, Hong KS, Lodewijks G. Anti-sway control of container cranes as a flexible cable system. Proceedings of the IEEE International Conference on Control Applications; Vol. 2, 2004. p. 1564–1569.
[14] Francis C, Mifdal A. Strong stability of a model of an overhead crane. Contr Cybern. 1998;27(3): 363–74.
[15] Hideki S. Boundary stabilization of hyperbolic systems related to overhead cranes. IMA J Math Contr Inf. 2008;25:353–66. doi:10.1093/imamci/dnm031.
[16] Boumedie'ne C, Han Z-J. On the stabilization of an overhead crane system with dynamic and delayed boundary conditions. IEEE Trans Automat Contr. 2019;65:4273–4280.
[17] D'Andrea-Novel B, Moyano I, Rosier L. Finite-time stabilization of an overhead crane with a flexible cable. Math Contr Signals Syst. 2019;31(2):1–19.
[18] Andrea-Noveland BD, Coron J-M. Stabilization of an over head crane with a variable length flexible cable. 2002.
[19] Moustafa KAF, Trabia MB, Ismail MI. Stability analysis and control of overhead crane with time-dependent flexible cable. Proceedings of 2005 IEEE/ASME International Conference on Advanced Intilligient Mechatronics; 2005.
[20] Nguyen TL, Do TH, Nguyen HQ. Vibration suppression control of a flexible gantry crane system with varying rope length. J Control Sci Eng. 2019;2019. doi:10.1155/2019/9640814.
[21] He W, Ge SS, Zhang S. Adaptive boundary control of a flexible marine installation system. Automatica. 2011;47(12):2728–2734.
[22] He W, Zhang S, Ge SS. Adaptive control of a flexible crane system with the boundary output constraint. IEEE Trans Indus Electr. 2014;61(8):4126–4133.
[23] He W, Ge SS. Cooperative control of a nonuniform gantry crane with constrained tension. Automatica. 2016;66:146–154.
[24] Nguyen TL, Duong MD. Nonlinear Control of Flexible Two-Dimensional Overhead Cranes. In: Adaptive robust control systems. Chapter 16, IntechOpen; 2016. p. 315–333.
[25] Tang Z-L, Tee KP, He W. Tangent barrier Lyapunov functions for the control of output-constrained nonlinear systems. IFAC Proc Vol. 2013;3(1):449–55. Elsevier Ltd, doi:10.3182/20130902-3-CN-3020.00122.